Visualizing White Matter Structure of the Brain using Dijkstra's Algorithm

Maarten H. Everts Henk Bekker Jos B.T.M. Roerdink
Institute of Mathematics and Computing Science
University of Groningen
Groningen, The Netherlands
{m.h.everts,h.bekker,j.b.t.m.roerdink}@rug.nl

Abstract

An undirected weighted graph may be constructed from diffusion weighted magnetic resonance imaging data. Every node represents a voxel and the edge weights between nodes represent the white matter connectivity between neighboring voxels. In this paper we propose and test a new method for calculating trajectories of fiber bundles in the brain by applying Dijkstra's shortest path algorithm to the weighted graph. Subsequently, the resulting tree structure is pruned, showing the main white matter structures of the brain. The time consumption of this method is in the order of seconds.

1 Introduction

The complexity of the human brain is enormous. In a volume of about 1.5 liter run some 10^5 kilometers of myelinated nerve fibers, connecting many cortical brain regions. Most of these fibers are grouped into fiber bundles of various widths. A single nerve fiber is a tube, with a diameter of typically one micron. Diffusion of water molecules in the longitudinal direction is free while transverse diffusion is limited. With diffusion-weighted magnetic resonance imaging (DW-MRI) the per-voxel averaged directional diffusion of water in biological tissue may be measured, resulting in a symmetric diffusion tensor $\mathbf{D}$ [1]. For a voxel in an area with well-aligned nerve fibers the largest eigenvector of $\mathbf{D}$ points in the main fiber direction. In the last decades DW-MRI has matured to the extent that it is now possible to use this modality for detecting and visualizing fiber bundles in the millimeter range. It has been used, for example, to build atlases of the brain [7], to study chronic brain diseases [15], and to assess acute stroke [11]. For an overview see [12] and [14].

In order to understand the functioning of the healthy or affected brain it is important that it is determined to which cortical regions fiber bundles connect and which trajectories they follow. Many techniques have been proposed that, starting from the tensor field, visualize DTI data. A simple approach is to visualize the fractional anisotropy (FA), a scalar quantity representing a certain ratio of the eigenvalues of $\mathbf{D}$. It is useful for visualizing white matter density. More demanding is (deterministic) *fiber tracking*, a technique to reconstruct and visualize fiber bundles. In the most straightforward approach trajectories are generated by following the direction of the greatest local eigenvector, starting from a given voxel [14]. Instead of only using the greatest eigenvector of $\mathbf{D}$, some methods use the entire diffusion tensor [10]. Also, level set methods have been applied [17], where the front propagates with a velocity depending on the eigenvectors of $\mathbf{D}$.

What these methods have in common is that the tensor field is interpreted as a way of *locally* describing the direction of highest velocity, and in fiber tracking this direction is followed. Alternatively, we propose to approach fiber tracking as a way of finding a lowest-weight path in a graph, which is constructed by connecting each voxel to its neighboring voxels with a weighted edge. The weights are defined such that paths that follow the principal diffusion direction have a low weight. Having a weighted graph, a minimum-weight fiber tract between two given points may be calculated using Dijkstra's algorithm [5]. In this paper we report on our experiments with this approach, called *shortest path fiber tracking* (SPFT). Dijkstra's algorithm does not simply give a single shortest path, but, for a given source voxel, a tree of shortest paths. This allows us to not only show a single shortest path, but also to produce an overview of white matter density, structure, and direction, by visualizing a pruned version of this tree. Furthermore we investigate a method to visualize SPFT results by clustering outer branches of the tree.

In the field of DTI visualization the SPFT method can be categorized as follows. In the first place it is a deterministic method; every run gives exactly the same result. However, it does not have the drawbacks of most other deterministic methods; paths are constructed using non-local information, yielding globally optimal paths. The paths generated by SPFT consist of edges connecting points of the voxel grid. This differs from most other methods, where paths are defined by non-grid points.

There are a few methods described in literature that also construct a graph from DW-MRI data and apply graph algorithms. In [8] an iterative adaptation of Dijkstra's algorithm is used to determine most probable paths between voxels

and to produce probabilistic brain anatomical connection maps. In a recent publication [20] a variation of Dijkstra's algorithm is used to compute optimal paths of maximum probability. The advantage of our method is its simplicity of assigning weights, and consequently its performance. On a similar dataset the method described in [20] is reported to take about 15 minutes, whereas our method runs in under 5 seconds. This makes our method suitable for interactive visualization.

The contribution of this paper can be summarized as follows. We present and test a new fiber tracking method, SPFT, that

- gives a fast (in the order of seconds) first impression of global white matter structure
- uses global information
- can be used for clustering.

In the following section we explain how the weighted graph is constructed and how the paths are created. Section 3 reports on experiments performed. In section 4 we discuss the advantages and disadvantages of our approach. Finally, in section 5 we conclude this paper and suggest possible future work.

2 Constructing a weighted graph and shortest paths from DTI data

Consider a diffusion tensor field $\mathbf{D}$ over the brain, where $\mathbf{D}_i$, $i = 1 \dots N$ is the diffusion tensor of voxel i and N the number of voxels. We assume that voxels are evenly spaced on a rectangular three-dimensional grid. Moreover, we assume that every diffusion tensor represents the average diffusion in the corresponding voxel, as measured by DW-MRI. In the following we use 26-connectedness, i. e., every voxel that is not at the boundary of the scanned volume has 26 neighboring voxels.

A mask is generated by using the brain extracting tool called `bet2` from the FSL package [16]. The mask is used to exclude areas without white matter, such as the skull and air surrounding the head. Also voxels in cerebrospinal fluid regions are excluded, characterized by a high value for the trace of the diffusion tensor. We used 9×10^{-4} as the maximum trace value.

A diffusion tensor $\mathbf{D}$ represents local diffusion, which means that the local flux $\mathbf{J}$ of particles, due to diffusion, over an infinitesimal plane A with unit normal $\mathbf{r}$ is given by the matrix-vector product

$$\mathbf{J} = \mathbf{D}\mathbf{r}. \tag{1}$$

In general $\mathbf{J}$ is not in the direction of $\mathbf{r}$. The flux $J_\mathbf{r}$ in the direction of $\mathbf{r}$ is given by

$$J_\mathbf{r} = \mathbf{r} \cdot \mathbf{D}\mathbf{r}. \tag{2}$$

Let $\mathbf{r}_{i,j} \equiv \mathbf{r}_j - \mathbf{r}_i$ and let $\hat{\mathbf{r}}_{i,j}$ be the corresponding unit vector, where $\mathbf{r}_i$ and $\mathbf{r}_j$ are the centers of voxels i and j, respectively. Using (2), and following the notation in [9], the diffusion coefficient in voxel i in the direction $\hat{\mathbf{r}}_{i,j}$ is denoted as

$$d(\mathbf{r}_{i,j}, i) \equiv \hat{\mathbf{r}}_{i,j} \cdot \mathbf{D}_i \hat{\mathbf{r}}_{i,j}. \tag{3}$$

According to [9] the connectedness C between two neighboring voxels i and j can be defined as

$$C_{i,j} = \frac{d(\mathbf{r}_{i,j}, i) + d(\mathbf{r}_{j,i}, j)}{2}. \tag{4}$$

For SPFT it is required that a high $C_{i,j}$ value is transformed into a low edge weight $W_{i,j}$. In order to enhance the effect of high C-values with respect to low values we use a nonlinear decreasing function S to map connectedness to weights:

$$W_{i,j} = S(C_{i,j}). \tag{5}$$

In our experiments we used a decreasing sigmoidal function of the form

$$S(x) = \frac{1}{1 + e^{a(x-b)}}, \tag{6}$$

where a is a positive constant that determines the steepness of the sigmoid and b is a constant that determines the x-position of the steepest point of S.

In our experiments we used $a = 15$, but any value in the range $14 \dots 16$ works just as well. The value of b differs per data set and is determined as follows. First, all $C_{i,j}$ are scaled to the range $0 \dots 1$ by dividing by the maximum of the C-values. Then, in the histogram of the C-values a value is chosen such that 98% is smaller, and b is set to this. The reason for this is that outliers in the C-values will otherwise influence the scaling too much and almost all weights of the graph would be near 1.0.

Dijkstra's algorithm [5] solves the single-source shortest path problem: given a weighted graph $G = (V, E)$, where V is a set of vertices and E a set of edges, find a shortest path from a given source vertex $s \in V$ to every vertex $v \in V$. A shortest path is defined as a path of which the sum of the weights of its edges, i. e., the path weight, is minimal. Dijkstra's algorithm returns for every vertex $v \in V$, the shortest path to s and the weight of the path. The shortest paths are represented by a *shortest path tree* where each vertex has a reference to a predecessor in the shortest path from that vertex to the source vertex. Note that Dijkstra's algorithm only works for graphs with non-negative edge weights. By implementing the priority queue used in Dijkstra's algorithm with a Fibonacci heap, the complexity of the shortest path algorithm becomes $O(|V| \log |V| + |E|)$, where $|E|$ is the number of edges and $|V|$ the number of vertices [4].

3 Results

The DT-MRI data used in this paper were acquired from a healthy volunteer on a 3T MRI system (Philips Intera). Diffusion Tensor Imaging was performed using a diffusion weighted spin-echo, echo-planar imaging technique. The

DTI parameters were as follows: 240×240 mm field of view; 128×128 matrix size; 51 slices; $1.85 \times 1.85 \times 2$ mm^3 imaging resolution; 5485 ms repetition time; 74 ms echo time. Diffusion was measured along 60 non-collinear directions. For each slice and each gradient direction, two images with no diffusion weighting ($b = 0$ s/mm^2) and diffusion weighting ($b = 800$ s/mm^2) were acquired, to measure APA and APP fat-shifts. The subject's consent was obtained prior to scanning. A tensor field was generated from the diffusion weighted data using the Diffusion Toolkit [19].

3.1 Visualization

The visualizations shown in this section were created using Python and the Visualization Toolkit (VTK). For better depth perception the paths and trees visualized are depicted using tubes with VTK's TubeFilter. In some of the images the paths are smoothed using approximating splines.

3.2 Single shortest path

A first step in visualizing SPFT results is to select one voxel in a region of interest and visualize its shortest path to the source voxel. This is illustrated in Figure 1, where a shortest path (red) is combined with a fiber tract produced by traditional deterministic fiber tracking (blue). The latter was created using a modified FACT [13] method provided by the `track` program of the Camino software package [3] and was seeded at the source voxel used for SPFT.

It can be seen that the SPFT path is very similar to the tract returned by the method for deterministic fiber tracking. The shortest path is not as smooth as the traditional fiber tract. This is partly because of the discretization necessary to be able to create a graph from the data. By interpolating the vertices of the shortest path by a spline the visual appearance can be improved. Note that in Figure 1 the shortest path is not smoothed to illustrate the jagged nature of the raw SPFT paths.

3.3 Visualizing brain structure

The next step after visualizing just one shortest path is visualizing the whole shortest path tree. This would of course create a very cluttered visualization, so instead we have experimented with visualizing a simplified, pruned tree and we propose two approaches for pruning. The first, pruning based on *tree size*, involves counting for each vertex the number of children in the shortest path tree. Then only those vertices are selected whose number of children in the shortest path tree are larger than a threshold t_{size}. The second approach, pruning based on *tree depth*, involves calculating for each vertex the maximum depth of the tree starting from that vertex, that is, the maximum path length to a leaf vertex in the tree. That value is then used for thresholding (t_{depth}). Both values, tree size and tree depth, are easily calculated recursively.

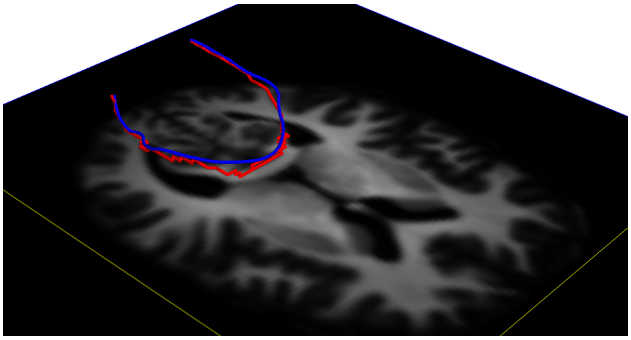

Figure 1. A shortest path (red) combined with a fiber tract from traditional deterministic fiber tracking (blue) seeded from the same voxel, shown together with a transverse plane showing fractional anisotropy for context. For the most part the tracts follow the same path.

Figures 2 to 6 show the results of applying pruning to the shortest path tree generated by SPFT. In these figures the pruned trees are smoothed using an approximating spline. A voxel near the brain stem is used as the source voxel. Figures 2 and 3 show the effect of the threshold parameter for both pruning based on size as well as depth. A large value (a), results in a very simple tree, and decreasing t_{size} and t_{depth} shows more and more detail ((b) and (c)).

In Figure 4 the pruned shortest path tree (size-based pruning) is shown together with image planes displaying fractional anisotropy (FA) information, where white means high FA. What we see here is that the edges of the pruned tree follow important white matter bundles to a reasonable approximation. This is also illustrated in Figure 5 where a transverse slice (four voxels thick) of a minimally pruned tree is combined with a plane showing FA information.

Of course the position of the source voxel influences what the resulting tree will look like. However, we found that when choosing two source voxels far apart, one near the brain stem and one in the corpus callosum, 72% of the edges of the shortest path trees match. Figure 6 shows what the pruned shortest path tree looks like when the source voxel is chosen in the corpus callosum.

3.4 Voxel clustering

Instead of constructing paths we can look at which voxels connect to the outer voxels of the pruned tree and perform clustering based on that information. This means that we cluster voxels together whose shortest paths to the source voxel go through the same voxel. This may give information on how certain regions are connected. Figure 7 shows a sagittal slice of colored clusters (a) and the same slice with FA information (b). For most regions in this image, the colored clusters match the white matter structure indicated by high FA values.

(a) $t_{\text{size}} = 1000$ (b) $t_{\text{size}} = 400$ (c) $t_{\text{size}} = 100$

Figure 2. Decreasing the threshold parameter for pruning based on tree size results in a visualization showing more detail.

(a) $t_{\text{depth}} = 25$ (b) $t_{\text{depth}} = 15$ (c) $t_{\text{depth}} = 10$

Figure 3. Decreasing the threshold parameter for pruning based on tree depth results in a visualization showing more detail.

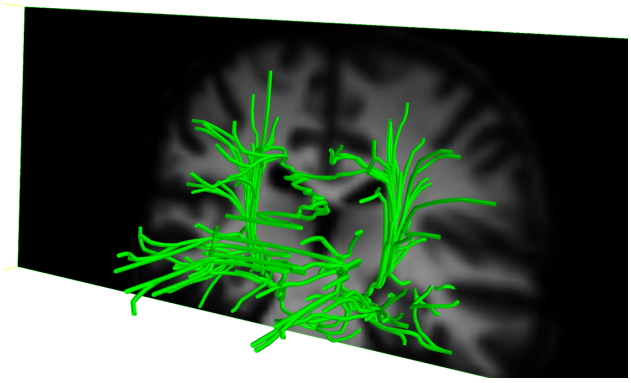

Figure 4. A pruned shortest path tree combined with a coronal plane showing fractional anisotropy. The tree shows the shape of part of the corpus callosum.

3.5 Path weight visualization

Besides a shortest path tree, Dijkstra's algorithm returns for each voxel the weight of the shortest path to the source voxel, which is basically a scalar field we can visualize. Figure 8 shows a sagittal slice of this weighted distance, colored using a red to yellow color scale. In addition we can calculate from the shortest path tree for each voxel the *length* of the path to the source voxel. Figure 9 shows this distance for the same sagittal slice. The neuroanatomical meaning and origin of the "parieto-occipital" red-yellow boundary in this figure is something that needs further analysis.

3.6 Performance

The graph construction and shortest path calculations are implemented in C, whereas the visualizations are created using a combination of Python and VTK.

Performance tests on a single core of an AMD Dual Opteron 280 (2.40 Ghz) were applied to a $128 \times 128 \times 51$ tensor field. The graph building process, which only needs to be done once, takes on average 1.2 seconds, and the shortest path calculation takes *on average 0.37 seconds*. Pruning the shortest path tree is implemented in Python and needs about 1 to 2 seconds.

4 Discussion

In our opinion SPFT should be considered as a fast fiber tracking method, both for previewing and interactive visualization. Computing time for the shortest path tree is under one second, so it is feasible to interactively change parameters to observe the effect. Even though the assignment of

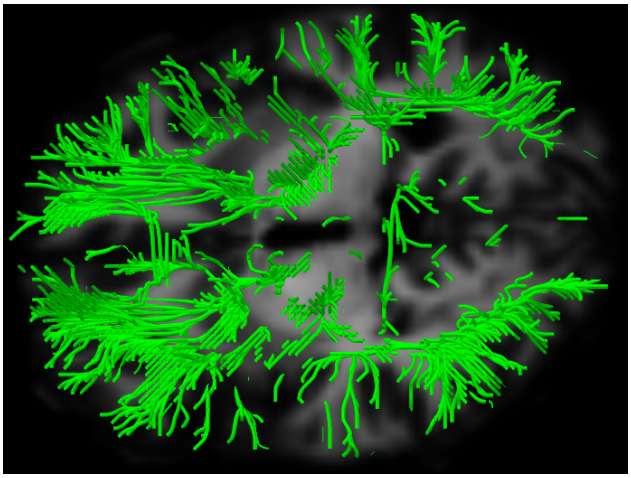

Figure 5. A 4-voxel thick transverse slice of a minimally pruned tree combined with a plane showing FA information.

Figure 6. Choosing a source voxel on the corpus callosum results in a pruned shortest path tree that is similar to the pruned tree found by using a source voxel near the brain stem (see for example Figure 2).

edge weights is simple, computing the shortest path tree already provides a good visual impression of brain structure.

This article is of the proof-of-principle type, i.e., further verification and validation is required. Notably a comparison with other methods has to be performed and the method should be tested on both healthy and pathological cases. Also, because of the noisy nature of DTI data, sensitivity to noise is something to be investigated. Preliminary testing showed that the shortest path tree only significantly changes after adding Gaussian noise with $\sigma > 0.1$.

An important issue is the interpretation of the edge weights. Although our initial edge assignment is based on diffusion densities, subsequent rescaling makes that it is not obvious what the ensuing minimization precisely means in neurophysiological terms. A more principled edge weight assignment can be based on probabilistic methods, like Bayesian estimation or Markov Chain Monte Carlo sampling. However, computation times of these all-paths tracking methods are much higher, ranging from 15 minutes [20], 30-40 minutes [6] to 18-24 hours [2]. An interesting open problem is to include the probabilistic edge assignment of Zalesky [20] in our method without increasing computation time too much.

Dijkstra's algorithm gives for every voxel pair a shortest path, even for voxel pairs that are not actually connected by a nerve fiber. Probably, such a path will have one or more relatively high weights. We tried to determine which paths represent real nerve fiber bundles and which ones are fictitious by comparing the highest single-step weight of the path with the average weight of the path. So far, this did not solve the problem.

5 Conclusion and Future Work

In this paper we have presented a new fast method for analyzing and visualizing DW-MRI data based on Dijkstra's shortest path algorithm. With this method one can quickly obtain an approximate overview of important white matter bundles or view paths between regions of interest. There is however, room for improvement. First of all, the computation of the edge weights needs some more theoretical underpinning to give meaning to what is actually minimized (see section 4). This can then be combined with a more extensive validation of the results produced by SPFT. Also, the tensor model has some known drawbacks with regard to crossing fibers and we will try to to combine other DW-MRI modalities such as Q-ball imaging [18] with SPFT. Finally, our current visualizations are very simple and there might be interesting innovative ways to explore the shortest path tree returned by SPFT or variants thereof.

Acknowledgements

We thank Cris Lanting and Pim van Dijk from the NeuroImaging Center in Groningen, The Netherlands for the brain dataset used in this paper. We also thank Alessandro Crippa for interesting discussions and test data. This research is part of the "VIEW" program, funded by the Dutch National Science Foundation (NWO), project no. 643.100.501.

References

[1] P. J. Basser, J. Mattiello, and D. LeBihan, "MR Diffusion Tensor Spectroscopy and Imaging.", *Biophysical Journal*, 66(1), Jan. 1994, pp. 259–267.

[2] T. Behrens, M. Woolrich, M. Jenkinson, H. Johansen-Berg, R. Nunes, S. Clare, P. Matthews, J. Brady, and S. Smith, "Characterization and Propagation of Uncertainty in Diffusion-Weighted MR Imaging", *Magnetic Resonance in Medicine*, 50(5), 2003, pp. 1077–1088.

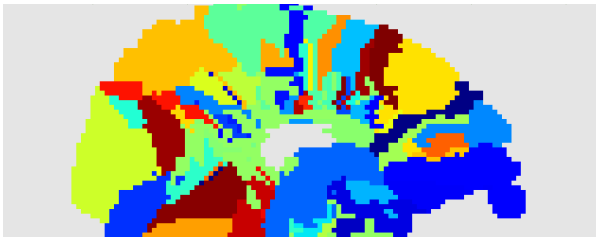

(a) Clusters

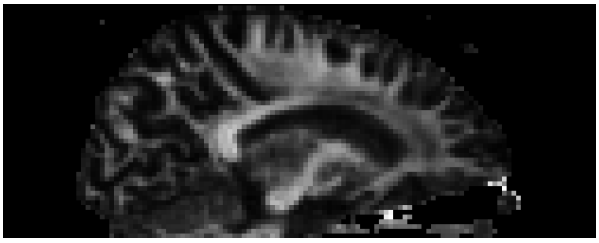

(b) FA

Figure 7. A sagittal slice showing colored clusters and a slice showing FA information. Most clusters align with the white matter structure shown in the FA map.

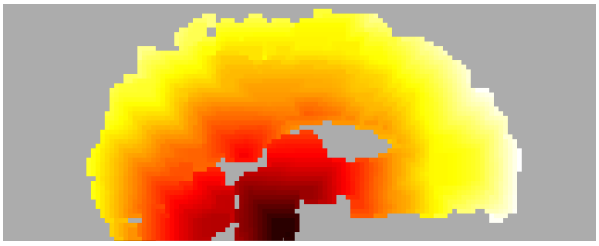

Figure 8. A sagittal slice showing for each voxel the weight of the shortest path to the source voxel.

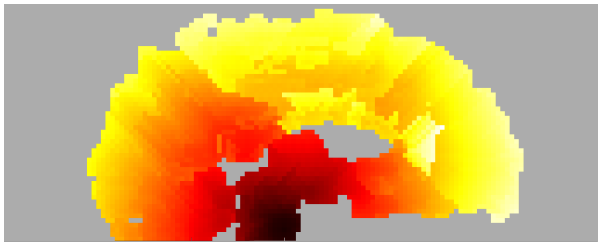

Figure 9. A sagittal slice showing for each voxel the length of the shortest path to the source voxel.

[3] P. Cook, Y. Bai, S. Nedjati-Gilani, K. K. Seunarine, M. G. Hall, G. J. Parker, and D. C. Alexander, "Camino: Open-Source Diffusion-MRI Reconstruction and Processing", In *Proc. ISMRM*, pp. 2759, Seattle, May 2006.

[4] T. H. Cormen, C. E. Leiserson, R. L. Rivest, and C. Stein, *Introduction to Algorithms*, The MIT Press, 2nd edition, Sept. 2001.

[5] E. W. Dijkstra, "A Note on Two Problems in Connexion With Graphs", *Numerische Mathematik*, 1(1), Dec. 1959, pp. 269–271.

[6] O. Friman, G. Farneback, and C.-F. Westin, "A Bayesian Approach for Stochastic White Matter Tractography.", *IEEE Transactions on Medical Imaging*, 25(8), Aug. 2006, pp. 965–978.

[7] P. Hagmann, J.-P. Thiran, L. Jonasson, P. Vandergheynst, S. Clarke, P. Maeder, and R. Meuli, "DTI Mapping of Human Brain Connectivity: Statistical Fibre Tracking and Virtual Dissection.", *NeuroImage*, 19(3), July 2003, pp. 545–554.

[8] Y. Iturria-Medina, E. J. Canales-Rodriguez, L. Melie-Garcia, P. A. Valdes-Hernandez, E. Martinez-Montes, Y. Aleman-Gomez, and J. M. Sanchez-Bornot, "Characterizing Brain Anatomical Connections Using Diffusion Weighted MRI and Graph Theory", *NeuroImage*, 36(3), July 2007, pp. 645–660.

[9] M. A. Koch, D. G. Norris, and M. Hund-Georgiadis, "An Investigation of Functional and Anatomical Connectivity Using Magnetic Resonance Imaging", *NeuroImage*, 16(1), May 2002, pp. 241–250.

[10] M. Lazar, D. M. Weinstein, J. S. Tsuruda, K. M. Hasan, K. Arfanakis, M. E. Meyerand, B. Badie, H. A. Rowley, V. Haughton, A. Field, and A. L. Alexander, "White Matter Tractography Using Diffusion Tensor Deflection.", *Human Brain Mapping*, 18(4), Apr. 2003, pp. 306–321.

[11] J. S. Lee, M.-K. Han, S. H. Kim, O.-K. Kwon, and J. H. Kim, "Fiber Tracking by Diffusion Tensor Imaging in Corticospinal Tract Stroke: Topographical Correlation With Clinical Symptoms.", *Neuroimage*, 26(3), July 2005, pp. 771–776.

[12] E. R. Melhem, S. Mori, G. Mukundan, M. A. Kraut, M. G. Pomper, and P. C. van Zijl, "Diffusion Tensor MR Imaging of the Brain and White Matter Tractography", *American Journal of Roentgenology*, 178(1), Jan. 2002, pp. 3–16.

[13] S. Mori, B. J. Crain, V. P. Chacko, and P. C. van Zijl, "Three-Dimensional Tracking of Axonal Projections in the Brain by Magnetic Resonance Imaging.", *Annals of Neurology*, 45(2), Feb. 1999, pp. 265–269.

[14] S. Mori and P. C. M. van Zijl, "Fiber Tracking: Principles and Strategies – A Technical Review.", *NMR in Biomedicine*, 15(7-8), Nov.–Dec. 2002, pp. 468–480.

[15] S. E. Rose, A. L. Janke, and J. B. Chalk, "Gray and White Matter Changes in Alzheimer's Disease: A Diffusion Tensor Imaging Study.", *Journal of Magnetic Resonance Imaging*, 27(1), Jan. 2008, pp. 20–26.

[16] S. M. Smith, M. Jenkinson, M. W. Woolrich, C. F. Beckmann, T. E. J. Behrens, H. Johansen-Berg, P. R. Bannister, M. De Luca, I. Drobnjak, D. E. Flitney, R. K. Niazy, J. Saunders, J. Vickers, Y. Zhang, N. De Stefano, J. M. Brady, and P. M. Matthews, "Advances in Functional and Structural MR Image Analysis and Implementation as FSL.", *NeuroImage*, 23 Suppl 1, 2004, pp. S208–19.

[17] J.-D. Tournier, F. Calamante, D. G. Gadian, and A. Connelly, "Diffusion-Weighted Magnetic Resonance Imaging Fibre Tracking Using a Front Evolution Algorithm.", *Neuroimage*, 20(1), Sept. 2003, pp. 276–288.

[18] D. S. Tuch, "Q-ball Imaging.", *Magnetic Resonance in Medicine*, 52(6), Dec. 2004, pp. 1358–1372.

[19] R. Wang and V. J. Wedeen. trackvis.org.

[20] A. Zalesky, "DT-MRI Fiber Tracking: A Shortest Paths Approach", *Medical Imaging, IEEE Transactions on*, 27(10), 2008, pp. 1458–1471.